FULL PAPER

Dalton
www.rsc.org/dalton

Reaction of metallophosphanide anions with ML$_n$X (X = halide) species as a simple route to heterometallic transition metal complexes

Birte Ahrens,[a,b] **Jacqueline M. Cole,**[a] **Jonathan P. Hickey,**[a] **James N. Martin,**[a] **Martin J. Mays,**[a]
Paul R. Raithby,[b] **Simon J. Teat**[c] **and Anthony D. Woods** *[a]
[a] *Department of Chemistry, University of Cambridge, Lensfield Road, Cambridge, UK CB2 1EW*
[b] *Department of Chemistry, University of Bath, Bath, UK BA2 7AY*
[c] *CLRC Daresbury Laboratory, Daresbury, Claverton Down, Warrington, UK WA4 4AD*

Received 13th November 2002, Accepted 19th February 2003
First published as an Advance Article on the web 4th March 2003

The reaction of metallophosphanides with ML$_n$X leads to the formation of mixed-metal clusters *via* complexes that consist of a metallophosphine coordinated through the lone pair on the phosphorus atom to another metal fragment. This synthetic strategy has been employed to initially form trinuclear complexes with the general formula [(Ph$_2$PML$_n$)(OC)$_2$Co(μ-DMAD)Mo(CO)$_2$Cp] (ML$_n$ = Mn(CO)$_5$ **3**, WCp(CO)$_2$ **4**, FeCp(CO)$_2$ **5**; DMAD = dimethylacetylenedicarboxylate) from the reaction of the anion [(Ph$_2$P)(OC)$_2$Co(μ-DMAD)Mo(CO)$_2$Cp]$^-$, **2**, with metal halide complexes, ML$_n$X (X = Cl, Br). The complexes **3**, **4** and **5** have been characterised spectroscopically, and an X-ray crystal structure of **5** shows that the Ph$_2$PFe(CO)$_2$Cp unit has coordinated to the cobalt centre through the lone pair on the phosphorus centre. Subsequent heating of **3** leads to carbonyl loss, and metal–metal bond formation, to yield [(OC)$_6$CpCoMnMo(μ-CO)(μ-PPh$_2$)(μ$_3$-η^2(//)-DMAD)], **6**. An X-ray structure determination of **6** confirms that it contains a 'closed' metal triangle. In a related series of reactions the cluster anion [Os$_3$(CO)$_{10}$(μ-PPh$_2$)]$^-$ was treated with a variety of metal-containing synthons, ML$_n$X. With [FeCp(CO)$_2$Cl] the cluster [Os$_3$(CO)$_{10}$FeCp(CO)(μ-PPh$_2$)(μ-CO)] **9** was obtained in good yield, and has been shown crystallographically to consist of an osmium triangle 'spiked' by an iron atom, with the Os–Fe bond bridged by the PPh$_2$ group and a carbonyl ligand. With [(Ph$_3$P)MCl] (M = Ag, Au) the tetranuclear 'butterfly' clusters [Os$_3$(CO)$_{10}$(μ-PPh$_2$)(μ-MPR$_3$)] (**10**: M = Au, R = Ph; **11**: M = Ag, R = Me) are obtained. These two complexes have been characterised spectroscopically and crystallographically.

Introduction

Interest in trimetallic species has grown for several reasons; including the possibility of using clusters as potential models for the chemisorption of unsaturated hydrocarbons on metallic surfaces.[1] More recently the catalytic properties of such trimetallic complexes have been studied with a view to organic synthesis[2] since heterometallic clusters should have additional enantio- and diastereoselective properties.[3] Investigating rational routes to heterometallic clusters, therefore, remains an active area of research. One strategy that is often employed in the preparation of such complexes is vertex exchange of isolobal metal fragments; such routes usually involve thermolysis with metal carbonyls, and unsurprisingly yields and product ratios are variable.[4]

The ability to introduce an additional metal fragment into the coordination sphere of a complex by bonding it to a two-electron donor that can substitute a carbonyl group seems a particularly appealing methodology. Metallophosphines such as [Ph$_2$PMoCp(CO)$_3$] are well known,[5] but these complexes are not particularly stable. They dimerize readily on heating, and often cannot be isolated in the solid state.[5,6] This precludes them from being used to add metal fragments to other complexes by simple substitution reactions, since the conditions required to effect substitution may also lead to dimerization of the phosphine and thus poor yields of the substituted complexes are obtained. Vahrenkamp and co-workers chose to use the metalloarsines, Me$_2$As[ML$_n$] in an attempt to circumvent the problem of dimerization and discovered a rational route to many tri- and tetra-nuclear clusters.[7–10] It seemed to us that a different strategy would be to substitute a metal complex with Ph$_2$PH, and then to deprotonate this phosphine in order to facilitate reaction with a different metal complex. Despite a growing interest in the reactivity of transition metal coordinated phosphanides towards many organic electrophiles over recent years,[11,12] there have been surprisingly few reactions of such phosphanides with metal salts.

Results and discussion

Deprotonation of a solution of [(Ph$_2$PH)(OC)$_2$Co(μ-DMAD)Mo(CO)$_2$Cp], **1**, with ^{n}BuLi proceeds smoothly at −78 °C to yield [(Ph$_2$P)(OC)$_2$Co(μ-DMAD)Mo(CO)$_2$Cp]$^-$ (DMAD = dimethylacetylendicarboxylate), **2**, which was used without any further purification in subsequent reactions.

Reactions with Mn(CO)$_5$, WCp(CO)$_2$ and FeCp(CO)$_2$

Stirring a THF solution of **2** with ML$_n$Cl at room temperature, for 1 h, gave one new orange product, [(Ph$_2$PML$_n$)(OC)$_2$Co(μ-DMAD)Mo(CO)$_2$Cp] (ML$_n$ = Mn(CO)$_5$, **3**; WCp(CO)$_2$, **4**; FeCp(CO)$_2$, **5**) in moderate to high yield (Scheme 1).

It was noted that solutions of **3** on being allowed to stand for several hours slowly turned green, and it was assumed that metal–metal bond formation was occurring to yield a metal triangle. In order to confirm this hypothesis it was decided to thermolyse a solution of **3**. Thus heating a toluene solution of **3** at 50 °C for 1 h led to the formation of a green solution. Separation by preparative TLC yielded green [(OC)$_6$CpCoMnMo(μ-CO)(μ-PPh$_2$)(μ$_3$-η^2(//)-DMAD)], **6**, in which metal–metal bond formation had occurred (// signifies parallel coordination).

Somewhat surprisingly, closure of the metal triangles of **4** and **5** proved to be rather difficult; thus heating a toluene solution of **5** at 60 °C for 3h led to the isolation of brown [(OC)$_4$CpCoFeMo(μ-CO)(μ-PPh$_2$)(μ$_3$-η^2(//)-DMAD)], **7**, in low (15%) yield, and thermolysis of toluene solutions of **4** led only to decomposition (Scheme 2). It is assumed that it is harder to

DOI: 10.1039/b211243d

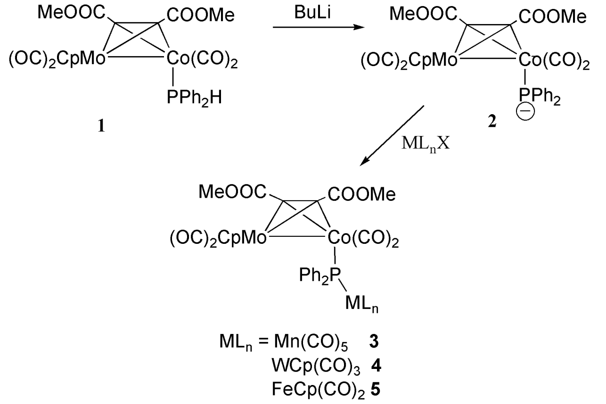

Scheme 1 Reaction of $[(Ph_2P)(OC)_2Co(\mu\text{-DMAD})Mo(CO)_2Cp]^-$, **2**, with metal salts.

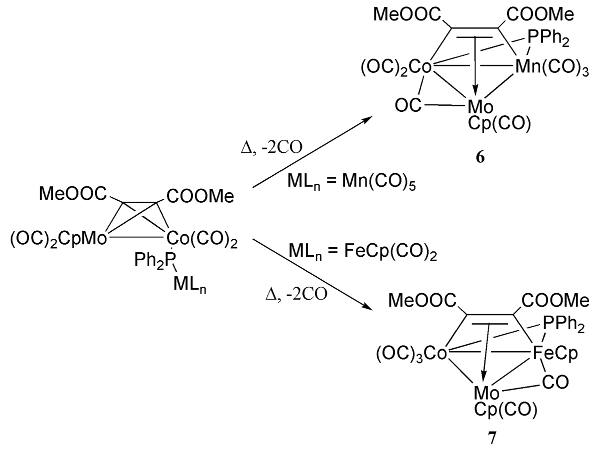

Scheme 2 Thermolysis of **3** and **5**.

cause the closure of the metal triangle for **4** and **5** because, as compared with **3**, the P–ML$_n$ fragment has less labile carbonyl ligands which can be displaced in order to permit metal–metal bond formation.

Complexes **3** to **7** have been characterised by IR, ^{1}H NMR, and ^{31}P NMR spectroscopy; satisfactory FAB MS and micro-analytical data were also obtained. Additionally **5** and **6** were characterised by single crystal X-ray diffraction studies. The molecular structure of **5** is shown in Fig. 1, with relevant bond lengths (Å) and angles (°) given in Table 1.

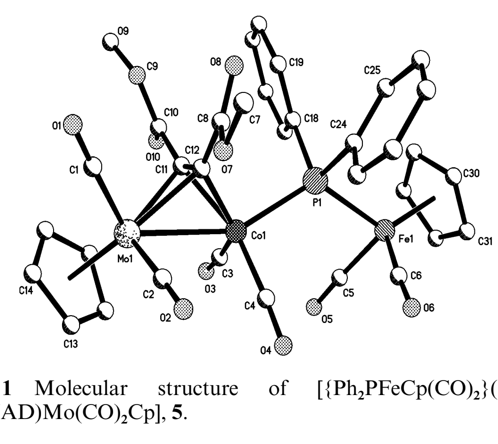

Fig. 1 Molecular structure of $[\{Ph_2PFeCp(CO)_2\}(OC)_2Co(\mu\text{-DMAD})Mo(CO)_2Cp]$, **5**.

The alkyne is coordinated transverse to the Mo–Co vector as expected for a μ-η^2 donor. The bond lengths and angles are all in the normal range for such core geometries.[13,14] Using the Wade–Mingos electron counting scheme[15] the core of **5** may be described as a *nido*-M_2C_2 cluster (based on the removal of one vertex from a trigonal bipyramid).

Table 1 Selected bond lengths (Å) and angles (°) for **5**

Mo(1)–Co(1)	2.6924(5)	Mo(1)–C(11)	2.169(3)
Mo(1)–C(12)	2.187(3)	Co(1)–C(11)	1.929(3)
Co(1)–C(12)	1.968(3)	Co(1)–P(1)	2.2794(9)
C(11)–C(12)	1.358(4)	Fe(1)–P(1)	2.3266(9)
Mo(1)–Co(1)–C(12)	53.27(8)	Mo(1)–C(11)–C(12)	72.5(2)
Mo(1)–C(11)–C(10)	121.2(2)	Mo(1)–C(11)–Co(1)	81.9(1)
Mo(1)–C(12)–C(8)	133.7(2)	Mo(1)–C(12)–Co(1)	80.59(9)
Mo(1)–Co(1)–C(11)	52.91(9)	Mo(1)–Co(1)–P(1)	150.71(3)
Co(1)–C(11)–C(12)	71.1(2)	Co(1)–C(11)–C(10)	138.5(2)

Table 2 Selected bond lengths (Å) and angles (°) for **6**

Mo(1)–Co(1)	2.6351(9)	Mo(1)–Mn(1)	2.883(1)
Mo(1)–C(10)	2.210(3)	Mo(1)–C(11)	2.296(3)
Mo(1)–C(6)	1.974(5)	Mn(1)–Co(1)	2.7013(7)
Mn(1)–C(11)	1.999(3)	Mn(1)–P(1)	2.257(1)
Co(1)–C(10)	1.965(3)	C(10)–C(11)	1.394(5)
Co(1)–P(1)	2.1958(9)	Co(1)–C(6)	2.3245(4)
Mo(1)–C(10)–C(11)	75.4(2)	Mo(1)–C(10)–C(9)	118.6(2)
Mo(1)–C(10)–Co(1)	78.0(1)	Mo(1)–C(11)–C(12)	126.2(2)
Mo(1)–C(11)–C(10)	68.6(2)	O(6)–C(6)–Mo(1)	165.9(4)
O(7)–C(7)–Mo(1)	168.8(3)	Mn(1)–Mo(1)–C(10)	64.59(8)
Mn(1)–Mo(1)–C(11)	43.60(8)	Mn(1)–Co(1)–C(10)	71.2(1)
Mn(1)–C(11)–C(10)	108.7(2)	Mn(1)–C(11)–C(12)	123.4(2)
Co(1)–Mo(1)–C(11)	67.84(9)	Co(1)–Mo(1)–C(10)	46.84(8)
Co(1)–Mn(1)–C(11)	70.3(1)	Co(1)–C(10)–C(11)	109.7(2)
C(10)–C(11)–C(12)	125.9(3)	C(9)–C(10)–C(11)	125.3(3)

The crystal structure of $[(OC)_6CpCoMnMo(\mu\text{-CO})(\mu\text{-PPh}_2)(\mu_3\text{-}\eta^2(//)\text{-DMAD})]$, **6**, consists of well separated molecular units. The molecular structure of **6** is shown in Fig. 2, and relevant bond lengths (Å) and angles (°) are included in Table 2. Within the molecular structure the ligand geometry is well defined but the metal triangle is disordered in a 4 : 1 ratio with the Mn and Co atoms each occupying both 'lighter atom' metal sites, and the molybdenum occupying two sites separated by 0.63 Å. Because of the inability to locate any light atoms associated with the second (approximately 20%) orientation of the metal triangle except for a slight movement in the position of the carbon atoms of the bridging carbonyls in the plane of the metal triangle, only the structure of the major (*ca.* 80% orientation) of the complex will be discussed in any detail.

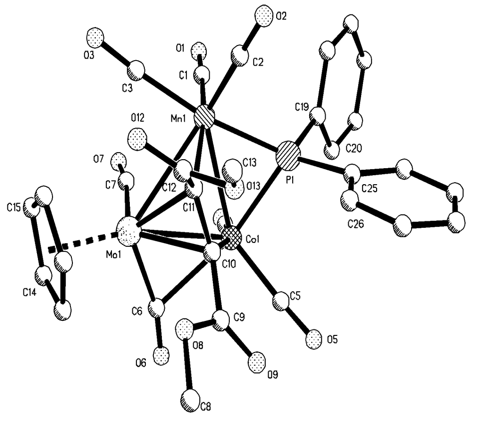

Fig. 2 Molecular structure of $[(OC)_6CpCoMnMo(\mu\text{-CO})(\mu\text{-PPh}_2)(\mu_3\text{-}\eta^2(//)\text{-DMAD})]$, **6**.

In **6** the alkyne is bound in μ_3-η^2-// fashion, with the η^2 coordination to the molybdenum atom being in accord with the work of Einstein.[16] The C(10)–C(11) vector is approximately parallel to the Co(1)–Mn(1) edge (3.1° deviation) with C(11) being located slightly closer to Mo(1). The dihedral angle between the Mn–P–Co and Mn–Co–Mo planes is 10.9° and that between the Mn–Co–Mo and Mo–Co–C(6) planes is 7.8°. Using the Wade–Mingos[15] electron counting scheme complex **6** can thus be described as a *nido*-M_3C_2 cluster possessing seven skeletal electron pairs. As such, the bond lengths and bond angles are of the same order of magnitude as those observed in other *nido* M_3C_2 clusters.[16] As is customary,[17] the M–C bonds in the *pseudo* square plane Mn–Co–C(10)–C(11) (maximum deviation from plane 0.0282 Å) are all shorter [C(11)–Mn(1) 1.999(3) Å, C(10)–Co(1) 1.965(3) Å] than those to the capping Mo unit [C(10)–Mo(1) 2.210(3) Å, C(11)–Mo(1) 2.296(3) Å]. It has previously been noted by Einstein *et al.*[16] that in such heterometallic square-based pyramids the thermodynamically preferred isomer has the most electron attracting fragments located in the 'basal' position, and the most electropositive metal at the apical site. Calculations have shown that this preference is based on a stronger bonding interaction between the alkyne and the two metals in the basal plane.[18] This proves to be true in the present case, with the Mo atom occupying the apical site of the square-based pyramid.

The formation of the metal triangle leads to an increase in the Co–Mo bond length from 2.6351(9) Å in **5** to 2.7059(6) Å in **6**. Unsurprisingly, the change in the mode of coordination of the alkyne from μ-η^2-$\perp$ to μ_3-η^2-// leads to a lengthening of the C(10)–C(11) bond length from 1.358(4) Å in **5** to 1.394(5) Å in **6** ($\perp$ signifies perpendicular coordination).

A semi-bridging carbonyl group is present on the molybdenum atom, as determined from the Mo–C(7)–O(7) bond geometry [Mo(1)–C(7)–O(7) 168.8(3)°]. The carbonyl carbon atom is in close contact with the two other metal centres [C(7)–Mn(1) 2.937 Å, C(7)–Co(1) 2.966 Å]. Semi-bridging carbonyl atoms are a common feature in hetero-trimetallic alkyne-bridged complexes. However, in the majority of these cases although the triangle electron count is the expected 48, the individual metals do not conform to the eighteen-electron rule.[16] It has been argued that in such cases the formation of a semi-bridging carbonyl group helps to offset the disparity between the formal individual electron counts of each metal centre.

Reactions of $[Os_3(CO)_{10}(\mu\text{-}PPh_2)]^-$ with $[ML_nX]$

In order to extend the general applicability of these reactions it was decided to investigate the reactivity of $[Os_3(CO)_{11}PPh_2H]$ **8** to M^+ synthons. Colbran and co-workers had previously demonstrated that **8** may be readily deprotonated but during this procedure a geometric change occurs yielding $[Os_3(CO)_{10}(\mu\text{-}PPh_2)]^-$ in which the phosphanide has adopted a bridging position; reprotonation thus yields $[Os_3(CO)_{10}(\mu\text{-}PPh_2)(\mu\text{-}H)]$.[19]

Treatment of a dichloromethane solution of **8** with DBU (DBU = 1,8-diazabicyclo[5.4.0]undec-7-ene) followed by addition of $FeCp(CO)_2Cl$ led to an immediate colour change from yellow to deep red to orange. Separation of the mixture by preparative TLC yielded one new product, $[Os_3(CO)_{10}FeCp(CO)(\mu\text{-}PPh_2)(\mu\text{-}CO)]$, **9**, in high yield (Scheme 3). Surprisingly, this proved to be the only reaction of its class which yielded isolable products. In contrast, the reaction of $[Os_3(CO)_{10}(\mu\text{-}PPh_2)]^-$ with $Mn(CO)_5Br$, $MCp(CO)_3Cl$ (M = Mo, W) and $RuCp(CO)_2Cl$ all appeared to proceed smoothly but the compounds decomposed during attempted chromatographic separation.

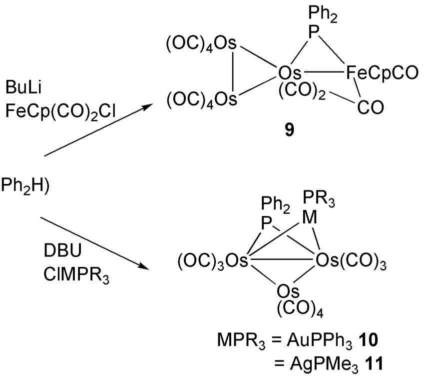

Scheme 3 Reaction of $Os_3(CO)_{11}(PPh_2H)$ with metal salts.

Table 3 Selected bond lengths (Å) and angles (°) for **9**

Os(1)–Os(2)	2.8686(14)	Os(2)–Os(3)	2.8924(16)
Os(1)–Os(3)	2.8736(13)	Os(3)–Fe(1)	2.7325(16)
Os(3)–P(1)	2.322(3)	Fe(1)–P(1)	2.199(3)
Os(1)–C(11)	1.970(9)	Fe(1)–C(11)	2.135(9)
Os(1)–Os(2)–Os(3)	59.84(4)	Os(1)–Os(3)–Os(2)	59.67(3)
Os(2)–Os(1)–Os(3)	60.49(4)	Os(3)–P(1)–Fe(1)	74.32(8)
Os(3)–C(11)–Fe(1)	83.4(4)	Os(1)–Os(3)–Fe(1)	152.18(6)
Os(2)–Os(3)–Fe(1)	147.41(5)		

The molecular structure of **9** was confirmed by a single-crystal X-ray diffraction study and is shown in Fig. 3, and relevant bond lengths (Å) and angles (°) are included in Table 3. The core consists of an iron spiked-Os_3 triangle, with the Fe–Os bond being bridged by a CO and PPh_2 group. Simple spiked Os_3 triangles are scarce, other examples being $[Os_3Pt(\mu\text{-}CH_2)(CO)_{11}(PPh_3)_2]$,[20] $[Os_4H_2(CO)_{15}]$,[21] $[Os_4H_3Br(CO)_{13}]$[22] and $[Os_4(CO)_{15}PMe_3]$.[23] The four metal atoms are not quite planar, the Fe atom lying 0.266 Å above the plane of the Os_3 triangle, with the dihedral angle between the Os_3 plane and $Os_1Os_3Fe_1$ plane being 8.9°; by contrast the dihedral angle between the planes in $[Os_4(CO)_{15}PMe_3]$ is 2.9°. The Os–Os bonds within the core [range 2.8686(14) to 2.8924(16) Å] compare closely with those in $[Os_3Pt(\mu\text{-}CH_2)(CO)_{11}(PPh_3)_2]$ [range 2.857(3) to 2.882(4) Å],[20] and to the average Os–Os bond length of 2.877 Å in $[Os_3(CO)_{12}]$.[24]

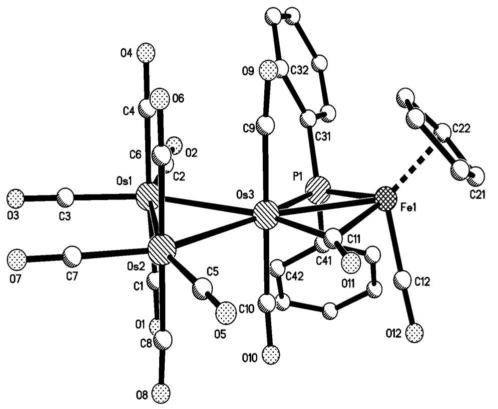

Fig. 3 Molecular structure of $[Os_3(CO)_{10}FeCp(CO)(\mu\text{-}PPh_2)(\mu\text{-}CO)]$, **9**.

The bulk of documented Fe–Os bonds are found either in mixed metal Fe_nOs_{3-n} triangles or as dative bonds between a bis-cyclopentadienyl coordinated Fe atom and an Os atom of an Os_3 triangle. Unsurprisingly, such dative bonds are long, being typically in the range of 2.813 to 2.995 Å,[25] whereas the mean Fe–Os separation in $[Fe_2Os(CO)_{12}]$ is 2.742 ± 0.005 Å,[26] both these separations being significantly longer than in the current case [Os–Fe 2.7325(16) Å]. The CO group bridging the Fe and an Os is asymmetric [Os(3)–C(11) 1.970(9) Å; Fe(1)–C(11) 2.135(9) Å]. Thus the Os–C separation is only marginally longer than that of a terminal Os–CO separation [range 1.88(1)–1.95(1) Å] whereas the Fe–C separation is significantly longer than the terminal Fe(1)–C separation of 1.756 (10) Å, although it is comparable with bridging Fe–C separations in $Fe_2Os(CO)_{12}$ [range 1.92(1) to 2.22(2) Å].[26]

Reactions with $[M(PR_3)Cl]$ [M = Ag, Au; R = Me, Ph]

The reaction of $[Os_3(CO)_{10}(\mu\text{-}PPh_2)]^-$ with $[MPR_3Cl]$ in the presence of Tl(OAc), which acts as a halide abstractor, led to the formation of $[Os_3(CO)_{10}(\mu\text{-}PPh_2)(\mu\text{-}MPR_3)]$ (**10**: M = Au, R = Ph; **11**: M = Ag, R = Me). This reaction may simply be

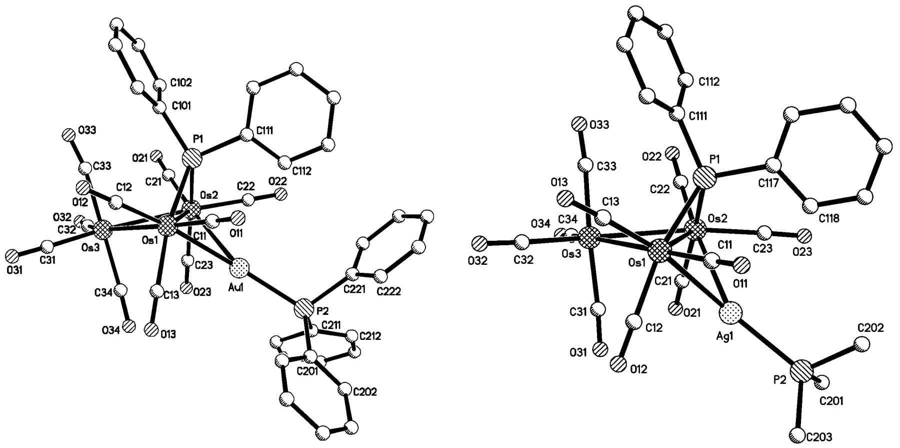

Fig. 4 Molecular structures of [$Os_3(CO)_{10}(\mu\text{-}PPh_2)(\mu\text{-}MPR_3)$] [**10**: M = Au, R = Ph (left); **11**: M = Ag, R = Me (right)].

Table 4 Selected bond lengths (Å) and angles (°) for **10**

Os(1)–Os(2)	2.9568(3)	Os(1)–Au(1)	2.7910(3)
Os(2)–Os(3)	2.8995(3)	Os(1)–Os(3)	2.8947(3)
Os(2)–Au(1)	2.7864(3)	Os(2)–P(1)	2.3643(13)
Os(1)–P(1)	2.3688(14)		
Os(1)–Os(2)–Os(3)	59.236(7)	Os(2)–Os(1)–Os(3)	59.395(7)
Os(1)–Os(3)–Os(2)	61.369(7)	Os(1)–Au(1)–Os(2)	64.030(7)
Os(1)–P(1)–Os(2)	77.32(4)		

Table 5 Selected bond lengths (Å) and angles (°) for **11**

Os(1)–Os(2)	2.9694(4)	Os(1)–Ag(1)	2.7802(7)
Os(2)–Os(3)	2.8829(4)	Os(1)–Os(3)	2.9068(4)
Os(2)–Ag(1)	2.8153(7)	Os(2)–P(1)	2.3712(19)
Os(1)–P(1)	2.3692(19)		
Os(1)–Os(2)–Os(3)	59.541(10)	Os(2)–Os(1)–Os(3)	58.749(10)
Os(1)–Os(3)–Os(2)	61.710(10)	Os(1)–Ag(1)–Os(2)	64.099(14)
Os(1)–P(1)–Os(2)	77.57(6)		

viewed as the isolobal analogue of the reaction reported by Colbran and co-workers.[19] Both complexes were characterised spectroscopically and in addition have been the subjects of single crystal X-ray diffraction studies (Fig. 4).

Complexes **10** and **11** consist of butterfly Os_3M cores in which the hinge Os–Os bond is bridged by a PPh_2 group. The dihedral angle of 113.1° between the Os_3 and Os(1)–Os(2)–P(1) planes of **10** is virtually identical to the value of 113.4° recorded in [$Os_3(CO)_{10}(\mu\text{-}PPh_2)(\mu\text{-}H)$],[27] but is larger than that in [$Os_3(CO)_9\{P(OMe)_3\}(\mu\text{-}H)(\mu\text{-}PPh_2)$][28] and [$Os_3(CO)_9(CF_3CO_2)_3(\mu\text{-}H)_2(\mu\text{-}PPh_2)$] (~110°).[29] The plane of the *endo*-Ph group in **10**, *i.e.* the Ph group lying above the Os_3 plane, lies approximately parallel to the Os(1)–Os(2) edge in order to minimise steric repulsion with the CO groups. However, its close proximity to the axial carbonyl of Os(3) [C(33)–$Ph_{centroid}$ 3.548 Å; O(33)–$Ph_{centroid}$ 3.028 Å] forces a marked deviation from the preferred linear CO geometry [Os(3)–C(33)–O(33) 169.6(6)°]. The *endo* and *exo* Ph groups are approximately perpendicular to each other; such a conformation has been assigned in similar structures by Deeming *et al.* on the basis of NMR spectroscopy studies.[30] The dihedral angle of 115.2° between the Os_3 and Os(1)–Os(2)–P(1) planes in **11** is larger than that in **10** presumably due to the lower steric demands of the bridging Ag–PMe_3 moiety. This greater dihedral angle manifests itself in a slightly lower distortion of the geometry of the axial CO groups [Os(3)–C(33)–O(33) 171.4(7)°] caused by the steric repulsion of the *endo*-Ph group of the μ-PPh_2 moiety. By comparison, the dihedral angle of 125.1° between the Os_3 and Os(1)–Os(2)–Ag(1) planes is significantly greater than the corresponding angle of 113.1° between the Os_3 and Os(1)–Os(2)–Au(1) planes in **10** thus supporting the argument that the smaller $AgPMe_3$ group creates less steric-repulsion. In both **10** and **11** the bridged Os–Os bond lengths are ~0.06 Å longer than the unbridged Os–Os bonds (see Tables 4 and 5) both of which are similar to the Os–Os bond lengths in [$Os_3(CO)_{12}$]. Furthermore the bridged bonds [**10**: 2.9568(3) Å, **11**: 2.9694(4) Å] are markedly longer than the corresponding separation of 2.916(1) Å in [$Os_3(CO)_{10}(\mu\text{-}H)(\mu\text{-}PPh_2)$]. It has been noted previously that the bond lengthening effect of a bridging coinage metal is greater than that of a bridging hydride.[31] To the authors' knowledge, despite several other Ag containing triangles being known, only one, the unsaturated cluster [$\{Os_3(CO)_{10}H\}_2Ag]^-$, has been crystallographically characterised.[32]

Gold bridged Os–Os bond lengths seem to be particularly dependent on the other ligands present. Thus the clusters [$Os_3(CO)_{10}(\mu\text{-}Cl)(\mu\text{-}AuPPh_3)$],[31] [$Os_6(CO)_{18}(\mu_6\text{-}P)(\mu\text{-}AuPPh_3)$][33] and [$Os_3(CO)_9(\mu\text{-}C_3H_5)(\mu\text{-}AuPEt_3)$][34] show bridged Os–Os separations of 2.880(2), 2.932(5) and 3.014(1) Å respectively *cf.* 2.9568(3) Å in **10**. The Os–Au separations in **10** fall within the normal range, and the Au fragment bridges symmetrically. The lack of similar structures incorporating Ag precludes any comparative discussion, although it is interesting to note that the bridged Os–Os bond length of **11** is 0.01 Å longer than that of **10** whereas in the two unsaturated compounds [$\{Os_3(CO)_{10}H\}_2Ag]^-$ and [$\{Os_3(CO)_{10}H\}_2Au]^-$ the corresponding bond length is 0.02 Å shorter in the Ag bridged complex.[32]

Conclusions

We have demonstrated that deprotonation of a coordinated PPh_2H moiety followed by reaction with a M^+ synthon represents a general method to introduce an additional metal fragment into the coordination sphere of a cluster. Such reactions frequently result on metal–metal bond formation and, as such, represent an excellent route to heterometallic compounds.

Experimental

Unless otherwise stated all experiments were carried out under an atmosphere of dry, oxygen-free nitrogen, using conventional Schlenk line techniques, and solvents freshly distilled from the appropriate drying agent. NMR spectra were recorded in $CDCl_3$ using a Bruker DRX 400 spectrometer, with TMS as an external standard for ^1H and ^{13}C spectra and H_3PO_4 as an external standard for ^{31}P NMR spectra. Infrared spectra were, unless otherwise stated, recorded in dichloromethane solution in 0.5 mm NaCl solution cells, using a Perkin Elmer 1710 Fourier Transform spectrometer. FAB mass spectra were obtained using a Kratos MS 890 instrument, using 3-nitrobenzyl alcohol as a matrix. Preparative TLC was carried out on 1 mm silica plates prepared at the University of Cambridge. Column chromatography was performed on Kieselgel 60

Table 6 X-Ray crystallographic data for the new complexes

Complex	**5**	**6**	**9**	**10**	**11**
Empirical formula	$C_{35}H_{28}Cl_2CoFeMoO_{10}P$	$C_{30}H_{21}CoMnMoO_{11}P$	$C_{32}H_{22}FeO_{12}Os_3P$	$C_{40}H_{25}AuO_{10}Os_3P_2$	$C_{25}H_{19}AgO_{10}Os_3P_2$
Weight	921.16	798.25	1255.92	1495.11	1219.81
Crystal system	Triclinic	Monoclinic	Monoclinic	Triclinic	Monoclinic
Space group	$P\bar{1}$	$P2_1/c$	$P2_1/c$	$P\bar{1}$	$P2_1/n$
a/Å	10.3658(4)	15.2152(5)	8.9577(19)	10.0320(2)	17.4362(2)
b/Å	10.7100(4)	10.9665(3)	10.834(2)	13.9040(2)	8.7998(1)
c/Å	18.1348(6)	19.4998(4)	34.169(7)	16.4300(4)	20.0377(3)
a/°	81.443(2)	90	90	94.6710(12)	90
β/°	80.052(2)	108.314(2)	94.537(10)	103.7790(9)	93.038(1)
γ/°	66.061(2)	90	90	111.1271(12)	90
V/Å^3	1805.49(11)	3088.9(2)	3305.7(12)	2040.47(7)	3070.17(7)
T/K	180(2)	180(2)	150(2)	180(2)	150(2)
Z	2	4	4	2	4
Abs coefficient/mm^{-1}	1.441	1.445	12.036	13.028	13.159
F(000)	924	1592	2316	1364	2216
Reflections measured	20615	25149	22341	26465	40543
Independent reflections	8217	7053	8711	8336	7038
R_{int}	0.0704	0.0606	0.0430	0.0666	0.0655
Final R_1, wR_2	0.0411, 0.0760	0.0436, 0.0877	0.0559, 0.0935	0.0333, 0.0857	0.0488, 0.1186
R_1, wR_2 (all data)	0.0779, 0.1034	0.0649, 0.3235	0.0786, 0.0973	0.0368, 0.0880	0.0578, 0.1411

(70–230 mesh ASTM). Unless otherwise stated, all reagents were obtained from commercial suppliers and used without further purification. [$(Ph_2PH)(OC)_2Co(\mu\text{-}DMAD)Mo(CO)_2Cp$],[14] [$Os_3(CO)_{11}(PPh_2H)$],[19] [$CpW(CO)_3Cl$][35] and [$CpFe(CO)_2Cl$][36] were prepared by the literature methods.

Crystal structure determinations

Single-crystal X-ray diffraction data for **5**, **6**, **10** and **11** were collected using a Nonius-Kappa CCD diffractometer, equipped with an Oxford Cryosystems cryostream and employing MoKα (0.71069 Å) irradiation from a sealed tube X-ray source. Cell refinement, data collection and data reduction were performed with the programs DENZO[37] and COLLECT[38] and multi-scan absorption corrections were applied to all intensity data with the program SORTAV.[39] The crystal structure of **9** was determined using the single-crystal diffraction Station 9.8 at the Synchrotron Radiation Source, Daresbury, UK. This houses a Bruker SMART diffractometer, equipped with an Oxford Cryosystems cryostream. A Si(111) monochromator enabled X-ray irradiation of $\lambda = 0.6923$ Å onto the sample. Cell refinement and data collection were performed using the SMART[40] software whilst the SAINT[41] and SADABS[42] programs were used for data reduction and absorption correlations respectively. All structures were solved and refined with the programs SHELXS97 and SHELXL97,[43] respectively. The structures of **6** and **9** show disorder. In **6** two positions of the Mo(1) atom were observed in an approximately 4 : 1 ratio. The two positions were refined with the total occupancy of the site summing to unity. Also, it was not possible to distinguish between the Mn and Co sites, and partial occupancies of each atom type were assigned to each position, with the atom positions of the Mn and Co atoms on each site constrained to be the same; again the partial occupancies on each site summed to unity. Slight differences in the position of the carbon atom of the bridging carbonyls, C(3) and C(6), in the plane of the metal triangle were also noted, and refined in conjunction with the difference in the Mo atom position using the same occupancy ratio. In the structure of **9** the Os triangle was disordered in a 96 : 4 ratio, with the low occupancy triangle showing a slight rotation about an approximate three-fold axis perpendicular to the triangle compared to the major component. Related Os atom sites were refined with the occupancies summed to unity. Because of the relative weakness of the data additional restraints were placed on the phenyl and cyclopentadienyl rings in order to stabilise the refinement. The crystal structure of **9** also contains a molecule of hexane solvent in the lattice that was disordered across a centre of symmetry. This molecule was refined with appropriate bond length and angle constraints. A summary of data collection and data refinement details is given in Table 6.

CCDC reference numbers 197610–14.

See http://www.rsc.org/suppdata/dt/b2/b211243d/ for crystallographic data in CIF or other electronic format.

Preparation of [$(Ph_2P)(OC)_2Co(\mu\text{-}DMAD)Mo(CO)_2Cp$]$^-$, 2

To a solution of [$(Ph_2PH)(OC)_2Co(\mu\text{-}DMAD)Mo(CO)_2Cp$] (250 mg, 0.38 mmol) in THF (40 ml) at −78 °C was added 1.7 M ^{t}BuLi (0.25 ml, 1.1 eq) leading to an immediate colour change from orange to deep brown to yield [$(Ph_2P)(OC)_2Co(\mu\text{-}DMAD)Mo\ (CO)_2Cp$]$^-$ **2**, which was used without further purification.

Reaction of 2 with $Mn(CO)_5Br$

To a solution of **2** (250 mg, 0.38 mmol) in THF (40 ml) at −78 °C was added $Mn(CO)_5Br$ (115 mg, 1.1 eq); the resulting solution was warmed to RT and stirred for 1 h. The solvent was removed *in vacuo*, the residue redissolved in the minimum of dichloromethane and applied to the base of TLC plates. Elution with 2 : 1 hexane/ethyl acetate yielded orange [$\{Ph_2PMn(CO)_5\}(OC)_2Co(\mu\text{-}DMAD)Mo(CO)_2Cp$], **3** (245 mg, 78%), as the sole product.

IR (ν CO/cm^{-1}): 2094 (w), 2019 (s), 1992 (s), 1963 (m), 1940 (m), 1913 (m); ^{1}H NMR δ: 7.81 to 7.34 (m, 10H, Ph), 3.53 (s, 6H, COOMe); ^{31}P NMR δ: 48.22 (s, br, Co–$\underline{P}Ph_2$Mn); FAB *m*/*z*: 854 M$^+$; M$^+$–nCO (n = 1 to 3); analysis calculated (found) for $CoMoMnC_{32}H_{21}O_{13}P$: C 45.21 (44.99), H 2.52 (2.47), P 3.58 (3.62).

Reaction of 2 with $CpW(CO)_3Cl$

Using an analogous procedure to that above **2** was reacted with $CpW(CO)_3Cl$ (132 mg, 1.1 eq) to give orange [$\{Ph_2PWCp(CO)_3\}(OC)_2Co(\mu\text{-}DMAD)Mo(CO)_2Cp$] (164 mg, 44%). IR ($\nu$ CO/cm^{-1}): 2007 (vs), 1964 (vs); ^{1}H NMR δ: 7.7–7.2 (m, 10H, Ph), 5.35 (s, 5H, Cp), 3.5 (s, 3H, COOMe), 3.3 (s, 3H, COOMe); ^{31}P NMR δ 38.7; FAB *m*/*z*: 1029 M$^+$, M$^+$–nCO (n = 1 to 3); analysis calculated (found) for $CoMoWC_{35}H_{26}O_{11}$: C 40.38 (40.90), H 2.46 (2.55), P 3.06 (3.01).

Reaction of 2 with $CpFe(CO)_2Cl$

Using an analogous procedure to that in the above reaction 250 mg of **2** was treated with $CpFe(CO)_2Cl$ (90 mg, 1.1 eq) to yield red [$\{Ph_2PFeCp(CO)_2\}(OC)_2Co(\mu\text{-}DMAD)Mo(CO)_2Cp$], **5** (292 mg, 92%), as the sole product. IR (ν CO/cm^{-1}): 2054 (w), 2033 (m), 2014 (s), 1991 (vs), 1980 (s), 1956 (m), 1948 (m); ^{1}H NMR δ: 7.70–7.10 (m, 10H, Ph), 5.25 (s, 5H, Mo–Cp), 4.85 (s, 5H, Fe–Cp), 3.50 (s, 6H, COOMe); ^{31}P NMR δ: 52.31 (s, br, Co–$\underline{P}$Ph$_2$Fe); FAB *m*/*z*: 836 M$^+$, M$^+$–*n*CO (*n* = 1 to 6); analysis calculated (found) for CoMoFeC$_{34}$H$_{26}$O$_{10}$: C 48.84 (48.74), H 3.13 (3.67), P 3.72 (3.70).

Reaction of 2 with Mn(CO)$_5$Br at 50 °C

Following the above procedure but heating the reaction at 50 °C for 1.5 h and work up by the above method gave orange [{Ph$_2$PMn(CO)$_5$}(OC)$_2$Co(μ-DMAD)Mo(CO)$_2$Cp], **3** (25 mg, 8%), and green [(OC)$_6$CpCoMnMo(μ-CO)(μ-PPh$_2$)(μ$_3$-η^2(//)-DMAD)], **6** (140 mg, 46%). IR (*ν* CO/cm^{-1}): 2054 (m), 2013 (s), 1998 (s), 1953 (s), 1941 (s), 1882 (w, br); ^{1}H NMR δ: 8.15–7.49 (m, 10H, Ph), 5.03 (s, 5H, Cp), 3.75 (s, 3H, COOMe), 3.64 (s, 3H, COOMe); ^{31}P NMR δ: 57.00 (s, vbr, CoMnμ-$\underline{P}$Ph$_2$); FAB *m*/*z*: 798 M$^+$, M$^+$–*n*CO (*n* = 1, 3 to 7); analysis calculated (found) for CoMoMnC$_{30}$H$_{21}$O$_{11}$P: C 45.80 (45.14), H 2.80 (2.65), P 3.86 (3.88).

Thermolysis of [{Ph$_2$PFeCp(CO)$_2$}(OC)$_2$Co(μ-DMAD)-Mo(CO)$_2$Cp], 5

A solution of **5** (100 mg, 0.12 mmol) in toluene (50 ml) was heated at 60 °C for 3 h. The solvent was removed *in vacuo*, the residue redissolved in the minimum of dichloromethane and applied to the base of TLC plates. Elution with 2 : 1 hexane/ethyl acetate yielded brown [(OC)$_3$Cp$_2$CoFeMo(μ-CO)(μ-PPh$_2$)-(μ$_3$-η^2(//)-DMAD)], **7** (14 mg, 15%), as the sole isolable product. IR (*ν* CO/cm^{-1}): 2012 (vs), 1990 (s), 1950 (m), 1940 (s), 1883 (m); ^{1}H NMR δ: 7.73–7.20 (m, 10H, Ph), 5.45 (s, 5H, Mo–Cp), 5.18 (s, 5H, Fe–Cp), 3.86 (s, 3H, COOMe), 3.57(s, 3H, COOMe); ^{31}P NMR δ: −27.14 (s, CoFeμ-$\underline{P}$Ph$_2$); FAB *m*/*z*: 780 M$^+$, M$^+$–*n*CO (*n* = 4, 5); analysis calculated (found) for CoMoFeC$_{32}$H$_{26}$O$_8$: C 49.33 (49.26), H 3.30 (3.36), P 3.95 (3.96).

Reactions of [Os$_3$(CO)$_{11}$(PPh$_2$H)], 8

To a solution of [Os$_3$(CO)$_{11}$(PPh$_2$H)], **8** (0.091g, 0.086 mmol), in THF (50 ml) was added 1.6M BuLi (0.06 ml, 1.1 eq) at −78 °C, an instantaneous colour change from yellow to red occurred. The solution was allowed to warm to RT during which time the colour changed to yellow. The reaction mixture was then cooled to −78 °C and CpFe(CO)$_2$Cl (20 mg, 1.1 eq) was added and the reaction mixture allowed to warm to RT during which time the colour changed from yellow to red. The solvent was removed *in vacuo*, the residue redissolved in the minimum of CH$_2$Cl$_2$ and applied to the base of TLC plates. Elution with 2 : 1 hexane/ethyl acetate yielded unreacted **8**, Cp$_2$Fe$_2$(CO)$_4$ and [Os$_3$(CO)$_{10}$FeCp(CO)(μ-PPh$_2$)(μ-CO)], **9** (75 mg, 72%).

IR (*ν* CO/cm^{-1}): 2102 (m), 2058 (sh), 2050 (ms), 2029 (sh), 2014 (s), 1983 (ms), 1939 (w); ^{1}H NMR δ: 7.74–7.36 (m, 10H, Ph) 4.61 (s, 5H, Cp); ^{31}P NMR δ: 87.30 (s, μ-PPh$_2$); FAB *m*/*z*: 1217 MH$^+$; M$^+$–*n*CO (*n* = 1 to 3); analysis calculated (found) for Os$_3$FeC$_{29}$H$_{15}$O$_{12}$P: C 28.86 (29.01), H 1.40 (1.21), P 2.46 (2.50).

Reaction of 8 with ClMPR$_3$

To a solution of [Os$_3$(CO)$_{11}$(PPh$_2$H)], **8** (0.091g, 0.086 mmol), in dichloromethane (50 ml) was added DBU (0.015 ml, 0.099 mol) at room temperature leading to an instantaneous colour change from yellow to red. After several minutes the solution reverted to its original colour. Addition of 1.1 eq of the relevant metal salt and 23 mg (1.1 eq) TlOAc resulted in an immediate colour change to red. The reaction mixture was stirred for a further 2 h. The solvent was removed *in vacuo*, the residue redissolved in the minimum of CH$_2$Cl$_2$ and applied to the base of TLC plates. Elution with 2 : 1 hexane/ethyl acetate yielded unreacted **8** and [Os$_3$(CO)$_{10}$(μ-PPh$_2$)(μ-AuPPh$_3$)], **10** (70 mg, 52%), or [Os$_3$(CO)$_{10}$-(μ-PPh$_2$)(μ-AgPMe$_3$)], **11** (20 mg, 19%).

Data for 10

IR (*ν* CO/cm^{-1}): 2088 (m), 2027 (s), 2005 (ms), 1977 (sh), 1958 (m); ^{1}H NMR δ: 7.98–7.04 (m, 25H, Ph); ^{31}P NMR δ: 132.26 (s, μ-PPh$_2$); FAB *m*/*z*: 1498 M$^+$, M$^+$–*n*CO (*n* = 1 to 6); analysis calculated (found) for Os$_3$AuC$_{40}$H$_{25}$O$_{10}$P$_2$: C 32.01 (32.13), H 1.64 (1.69), P 4.22 (4.14).

Data for 11

IR (*ν* CO/cm^{-1}): 2155 (w), 2125 (w), 2086 (m), 2054 (mw), 2018 (s), 2003 (ms), 1973 (sh), 1951 (m), 1945 (m); ^{1}H NMR δ: 6.95–8.12 (m, 10H, Ph), 1.49 (d, 9H, Me); ^{31}P NMR δ: 71.02 (s, μ-PPh$_2$), 18.88 (s, 1P, PMe$_3$); FAB *m*/*z*: 1222 MH$^+$; analysis calculated (found) for Os$_3$AgC$_{25}$H$_{19}$O$_{10}$P$_2$: C 25.00 (24.61), H 1.68 (1.57), P 5.04 (5.08).

Acknowledgements

We acknowledge the financial support of the EPSRC (J.N.M., A.D.W. and for the purchase of the Nonius Kappa CCD diffractometer). A.D.W. and J.M.C. are grateful to St Catharine's College, Cambridge, for the award of Research Fellowships and additionally, J.M.C. thanks the Royal Society for a University Research Fellowship. The award of a DAAD grant (Gemeinsames Hochschulsonderprogramm III von Bund und Ländern) to B.A. is gratefully acknowledged. Dr John E. Davies is thanked for crystal structure determinations. Johnson Matthey PLC is thanked for the loan of metal salts.

References

1 P. R. Raithby and M. J. Rosales, *Adv. Inorg. Chem. Radiochem.*, 1985, **29**, 169 and references therein.
2 H. Adams, N. A. Bailey, L. J. Gill, M. J. Morris and N. D. Sadler, *J. Chem. Soc., Dalton Trans.*, 1997, 3041.
3 P. Braunstein and J. Rosé, in *Metal Clusters in Chemistry*, ed. P. Braunstein, L. A. Oro and P. R. Raithby, Wiley-VCH, 1999, vol. 2, p. 616.
4 Y.-B. Dong, Q. M. Hu, X. Y. Huang, L.-C. Song and J. Sun, *Organometallics*, 1997, **16**, 4540 and references therein.
5 I. J. Colquhoun, W. M. M^{c}Farlane, R. Maisch and W. Malisch, *J. Organomet. Chem.*, 1981, **220**, C1.
6 T. Adatia, M. M^{c}Partlin, M. J. Mays, M. J. Morris and P. R. Raithby, *J. Chem. Soc., Dalton Trans.*, 1989, 1555.
7 F. Richter and H. Vahrenkamp, *Angew. Chem., Int. Ed. Engl.*, 1979, **18**, 531.
8 R. Blumhofer, K. Fischer and H. Vahrenkamp, *Chem. Ber.*, 1986, **119**, 194.
9 F. Richter and H. Vahrenkamp, *Organometallics*, 1982, **1**, 756.
10 J. Ensling, K. Fischer, P. Gütlich, M. Müller, H.-T. Schacht and H. Vahrenkamp, *Inorg. Chem.*, 1986, **25**, 4032.
11 N. Gunzelmann, W. Malisch, F-J. Rehmann, J. Reising and K. Thirase, *Eur. J. Inorg. Chem.*, 1998, 1589.
12 J. E. Davies, N. Feeder, M. J. Mays, P. K. Tompkin and A. D. Woods, *Organometallics*, 2000, **19**, 984–993.
13 M. Gruselle, B. Malézieux and J. Vaissermann, *Organometallics*, 1998, **17**, 2337.
14 A. Martin, M. J. Mays, P. R. Raithby and G. A. Solan, *J. Chem. Soc., Dalton Trans.*, 1993, 1431.
15 D. M. P. Mingos and D. J. Wales, *Introduction to Cluster Chemistry*, Prentice Hall, New York, 1992; D. M. P. Mingos, *J. Chem. Soc., Dalton Trans.*, 1974, 133 and references therein.
16 F. W. B. Einstein, D. Sutton, A. S. Tracey and K. G. Tyers, *Inorg. Chem.*, 1986, **25**, 1631.
17 P. Bougeard, G. Jaouen, M. J. M^{c}Glinchey, A. Marinetti, M. Melkuz, J. B. Naceur, B. G. Sayer and J.-Y. Saillard, *Organometallics*, 1985, **4**, 1123.
18 J.-F. Halet, G. Jaouen, R. Lissillour, M. J. M^{c}Glinchey and J.-Y. Saillard, *Inorg. Chem.*, 1985, **24**, 218.
19 S. B. Colbran, B. F. G. Johnson, J. Lewis and R. Sorrell, *J. Organomet. Chem.*, 1985, **296**, C1.
20 G. L. Geoffroy, M-C. Lieszkovszky, C. A. Mirkin, A. L. Rheingold and G. D. Williams, *Organometallics*, 1986, **5**, 2228.
21 E. J. Ditzel, D. H. Holden, B. F. G. Johnson, J. Lewis, A. Saunders and M. J. Taylor, *J. Chem. Soc., Chem. Commun.*, 1982.

22 E. J. Ditzel, B. F. G. Johnson, J. Lewis, P. R. Raithby and M. J. Taylor, *J. Chem. Soc., Dalton Trans.*, 1985, 555.

23 F. W. B. Einstein, L. R. Martin and R. K. Pomeroy, *Organometallics*, 1988, **7**, 294.

24 M. R. Churchill and B. DeBoer, *Inorg. Chem.*, 1977, **16**, 878.

25 W. R. Cullen, S. J. Rettig and T-C. Zhang, *Organometallics*, 1992, **11**, 277.

26 M. R. Churchill and J. C. Fettinger, *Organometallics*, 1990, **9**, 446.

27 C. E. Housecroft, B. F. G. J. Johnson, J. Lewis, E. Nordlander and P. R. Raithby, *Inorg. Chim. Acta*, 1997, **259**, 345.

28 S. B. Colbran, P. T. Irele, B. F. G. Johnson, F. J. Lahoz, J. Lewis and P. R. Raithby, *J. Chem. Soc., Dalton Trans.*, 1989, 2023.

29 S. B. Colbran, P. T. Irele, B. F. G. Johnson, F. J. Lahoz, J. Lewis and P. R. Raithby, *J. Chem. Soc., Dalton Trans.*, 1989, 2033.

30 A. J. Deeming, S. Doherty, M. W. Day, K. I. Hardcastle and H. Minassian, *J. Chem. Soc., Dalton Trans.*, 1991, 1273.

31 K. Burgess, N. E. Leadbeater, J. Lewis and P. R. Raithby, *New J. Chem.*, 1998, 757.

32 M. Fajardo, M. P. Gómez-Sal, H. D. Holden, B. F. G. Johnson, J. Lewis, R. C. S. McQueen and P. R. Raithby, *J. Organomet. Chem.*, 1984, **267**, C25.

33 S. B. Colbran, C. M. Hay, B. F. G. Johnson, F. J. Lahoz, J. Lewis and P. R. Raithby, *J. Chem. Soc., Chem. Commun.*, 1986, 1766.

34 C. E. Housecroft, B. F. G. Johnson, J. Lewis, J. A. Lunniss, S. M. Owen and P. R. Raithby, *J. Organomet. Chem.*, 1991, **409**, 271.

35 T. S. Piper and G. Wilkinson, *J. Inorg. Nucl. Chem.*, 1956, **3**, 104.

36 E. C. Johnson, T. J. Meyer and N. Winterton, *Inorg. Chem.*, 1971, **16**, 1673.

37 Z. Otwinowski and W. Minor, *Methods Enzymol.*, 1997, **276**, 307.

38 R. Hooft, *COLLECT*, Nonius BV, Delft, The Netherlands, 1998.

39 R. H. Blessing, *Acta Crystallogr.*, 1995, **A51**, 33.

40 SMART, Bruker AXS Inc., Madison, WI, USA, ver. 5.054, 1999.

41 SAINT, Bruker AXS Inc., Madison, WI, USA, ver. 6.02a, 2000.

42 G. M. Sheldrick, SADABS, Program for area detector adsorption correction, Institute for Inorganic Chemistry, University of Göttingen, Germany, 1996.

43 G. M. Sheldrick, SHELXS-97, Program for solution of crystal structures, University of Göttingen, Germany, 1997; G. M. Sheldrick, SHELXL-97, Program for refinement of crystal structures, University of Göttingen, Germany, 1997.